



# Electronic structure and band alignment of Blue Phosphorene/Janus ZrSSe heterostructure: A first principles study



Chuong V. Nguyen<sup>a</sup>, Vo T.T. Vi<sup>b</sup>, Le T.T. Phuong<sup>b</sup>, Bui D. Hoi<sup>b</sup>, Le T. Hoa<sup>c,d</sup>, Nguyen N. Hieu<sup>c,d</sup>, Huynh V. Phuc<sup>e</sup>, Pham D. Khang<sup>f,g,\*</sup>

<sup>a</sup> Department of Materials Science and Engineering, Le Quy Don Technical University, Ha Noi, Viet Nam

<sup>b</sup> Department of Physics, University of Education, Hue University, Hue, Viet Nam

<sup>c</sup> Institute of Research and Development, Duy Tan University, Da Nang 550000, Viet Nam

<sup>d</sup> Faculty of Natural Sciences, Duy Tan University, Da Nang 550000, Viet Nam

<sup>e</sup> Division of Theoretical Physics, Dong Thap University, Dong Thap, Viet Nam

<sup>f</sup> Laboratory of Applied Physics, Advanced Institute of Materials Science, Ton Duc Thang University, Ho Chi Minh City, Viet Nam

<sup>g</sup> Faculty of Applied Sciences, Ton Duc Thang University, Ho Chi Minh City, Viet Nam

## ARTICLE INFO

### Keywords:

Blue Phosphorene  
Janus ZrSSe  
DFT calculations  
van der Waals heterostructures  
Band alignment

## ABSTRACT

In this work, we construct the BlueP/ZrSSe heterostructure and explore systematically its electronic characteristics and interface features in the framework of first principles calculations. The stacking and electric field effects on the interface characters of BlueP/ZrSSe heterostructure are also considered. We find that the BlueP layer interacts with Janus ZrSSe layer via the weak van der Waals forces, which keeps the BlueP/ZrSSe heterostructure feasible. Both the BlueP/SZrSe and BlueP/SeZrS heterostructures possess indirect semiconductor and exhibits type-I band alignment. Furthermore, electric field can tune the band alignment and switch the BlueP/ZrSSe heterostructure from semiconductor to metal. These findings could provide a helpful guidance for using BlueP/ZrSSe heterostructure in practical applications of nanoelectronics and optoelectronics.

## 1. Introduction

Last decade, the development of nanoscience and nanomaterials has motivated scientific community to search for novel materials with many intriguing properties. Owing to excellent electro-optical properties [1–3], graphene has been emerged a lot of considerable interest and opened up a new chapter for thin film two-dimensional (2D) materials, which can be considered as promising candidate for various applications, including optoelectronic, photocatalyst, gas sensors, light-emitting diodes [4–7]. To now, there are many 2D materials, including hexagonal boron nitride (hBN) [8,9], phosphorene [10,11], transition metal dichalcogenides (TMDCs) [12–16] and graphitic carbon nitrides [17,18] and others [19–22]. However, the most of 2D materials in their freestanding monolayers have a drawback that may hinder their applications in high-efficient devices. For instance, the lack of an electronic band gap in graphene makes it incompatible with high-speed logic circuit devices [23]. Molybdenum disulfide ( $\text{MoS}_2$ ) is one of the most famous TMDCs, it exhibits a semiconducting nature with a suitable band gap of about 2 eV for semiconductor energy devices [24]. Unfortunately, due to a small carrier mobility of about  $200 \text{ cm}^2/\text{Vs}$ ,

$\text{MoS}_2$  monolayer is incompatible with high-performance nanoelectronic devices [25]. Therefore, along with the design and synthesis of new 2D materials, one of the most important tasks for research on 2D materials is how to tune the properties and extend the range of applications of these 2D materials.

More recently, an another method that has currently been investigated is constructing layered heterostructures between two or more different 2DMs. Layers of 2DMs are stacked together result in the formation of a large electric field, originating from the difference in their work functions. Both theoretical and experimental studies demonstrated that these layered heterostructures are bonded via the long-range forces, which are kept the systems feasible and they can easily fabricate in practical applications [26–29]. Nowadays, there have been many different heterostructures have been created by stacking 2DMs above on top of others, such as graphene/2DMs [30–35], TMDCs heterostructures [36–43], and others [44]. All these above studies demonstrate that layered heterostructures based on two or more 2DMs are promising candidate for novel high-efficiency optoelectronics and nanoelectronics.

\* Corresponding author.

E-mail addresses: [chuongnguyen11@gmail.com](mailto:chuongnguyen11@gmail.com) (C.V. Nguyen), [phamdinhhkhang@tdtu.edu.vn](mailto:phamdinhhkhang@tdtu.edu.vn) (P.D. Khang).

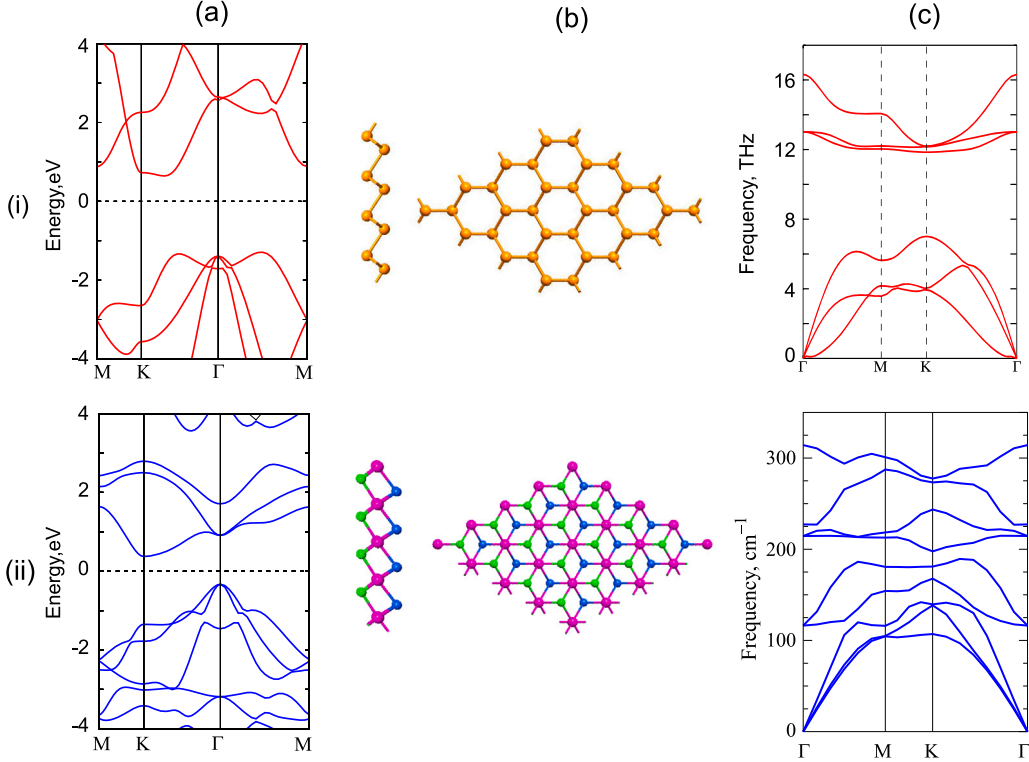


**Fig. 1.** (a) Band structure, (b) atomic structure and (c) phonon dispersion curves of (i) BlueP and (ii) Janus ZrSSe monolayer, respectively. The dashed black line in the band structures represent the Fermi level, which is set to be zero energy.

Very recently, a new type of 2DM phosphorus, namely blue phosphorene (BlueP), and TMDCs, namely Janus TMDCs have been successfully fabricated in recent experiments [45,46]. BlueP has a similar structure as silicene, which possesses the puckered hexagonal structure. Whereas, Janus TMDCs exhibit an intrinsic dipole moment because of the out-of-plane symmetry breaking. The electronic and optical properties of BlueP and TMDCs are very sensitive to other conditions, such as strain [47–50], functionalization [51–53], stacking layers [54–56]. Especially, the layered heterostructures between BlueP and different types of Janus TMDCs have been constructed and investigated [57,58]. For instance, Chen et al. [57] demonstrated that the BlueP/MoS<sub>2</sub> exhibits type-I or type-II band alignment, depending on the stacking configurations. Moreover, the strain and electric field can tune both the electronic features and interface characteristics of such heterostructures, making them suitable material for various applications. However, to our best knowledge, the electronic and interface characteristics of BlueP/Janus ZrSSe heterostructure have not yet been investigated previously. It should be noted that Janus ZrSSe monolayer has not yet been synthesized experimentally. However, the Janus TMD monolayer MoSSe has been successfully synthesized by sulfurization of monolayer MoSe<sub>2</sub> [59] or by selenization of monolayer MoS<sub>2</sub> [46]. Additionally, single layer ZrS<sub>2</sub> has been successfully synthesized experimentally through an electrochemical lithiation process [60]. Therefore, we believe that Janus ZrSSe monolayer can also be synthesized in the near future by selenization of monolayer ZrS<sub>2</sub>.

Therefore, in this work, we construct the BlueP/ZrSSe heterostructure and examine its electronic and interface characteristics using first principles calculations. We find that the BlueP/Janus ZrSSe heterostructures exhibit type-I band alignment and display the indirect band gap nature of semiconductor at the equilibrium state. The interface properties of such heterostructure can be modulated by applying electric field. The semiconducting character of such heterostructure can be converted into metallic one, making it acceptable for various applications of nanoelectronics and optoelectronics.

## 2. Computational methods

The calculations of the geometric structure and electronic characteristics of materials are performed by means of density functional theory (DFT) within Quantum Espresso [61,62]. To obtain the equilibrium geometric structures of considered systems, we use the generalized gradient approximation (GGA) from Perdew, Burke, and Ernzerhof (PBE) functional and projected augmented wave. For describing correctly the weak forces in layered systems of heterostructures, we use the long-range Grimme-D2 method [63]. A cut-off energy of 410 eV is used for the expansion of the plane-wave method. The force and energy convergence are set to be 0.001 eV/Å and 10<sup>-6</sup> eV, respectively. A vacuum of 35 Å is applied along the z direction of heterostructure to avoid all unphysical interactions. A 9 × 9 × 1 k-point mesh is sampled in the Monkhorst-Pack scheme of the Brillouin zone (BZ). The phonon dispersion curves of the constituent monolayers are calculated by using density functional perturbation theory with 27 × 27 × 1 k-point mesh. It should be noted that the accuracy of the lattice parameter of Blue P and Janus ZrSSe monolayers strongly depends on the chosen k-point mesh and cut-off energy. Thus, before constructing the heterostructure, we checked the accuracy of the obtained results by calculating the convergence of the total energy of both BlueP and Janus ZrSSe monolayers as a function of k-point mesh and cut-off energy. Our results demonstrate that the total energy of these 2D materials is converged at the cut-off energy of 410 eV and k-point mesh of (9 × 9 × 1). It indicates that the lattice constant does not show significant change (only of the order of ± 0.92%) when increasing the cut-off energy and k-point mesh, confirming the reliability of the computational parameters used in this work.

## 3. Results and discussion

We first examine and investigate the atomic structures and electronic characteristics of BlueP (BP) and Janus ZrSSe (JZ). The atomic

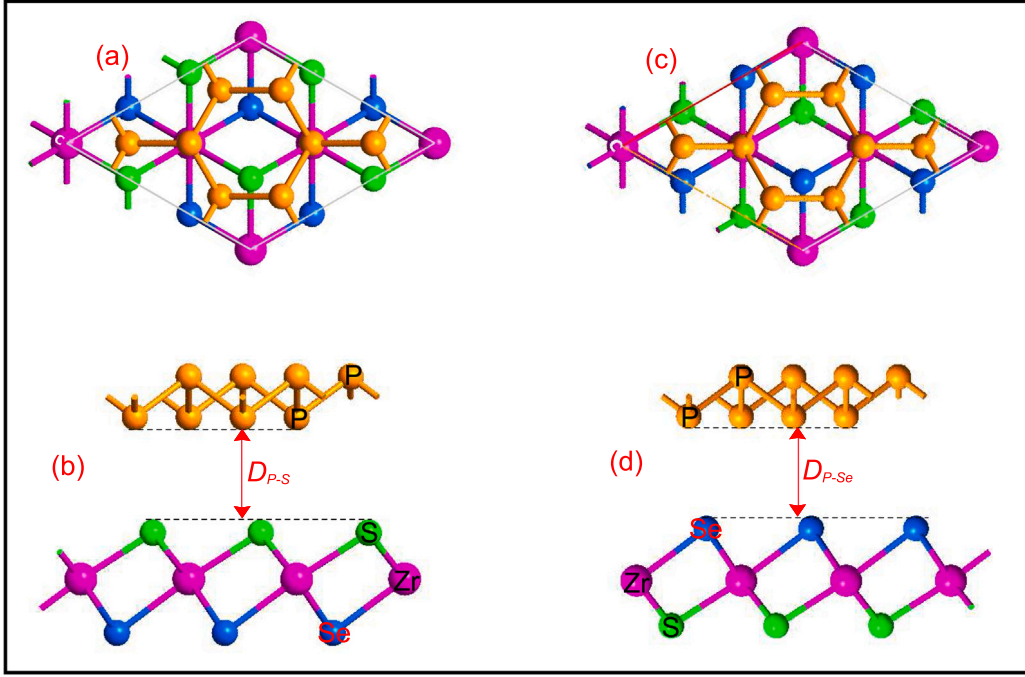


**Fig. 2.** (a, c) Top view and (b, d) side view of the relaxed atomic structure of (a, b) BP/SJZ and (c, d) BP/SeJZ heterostructures.

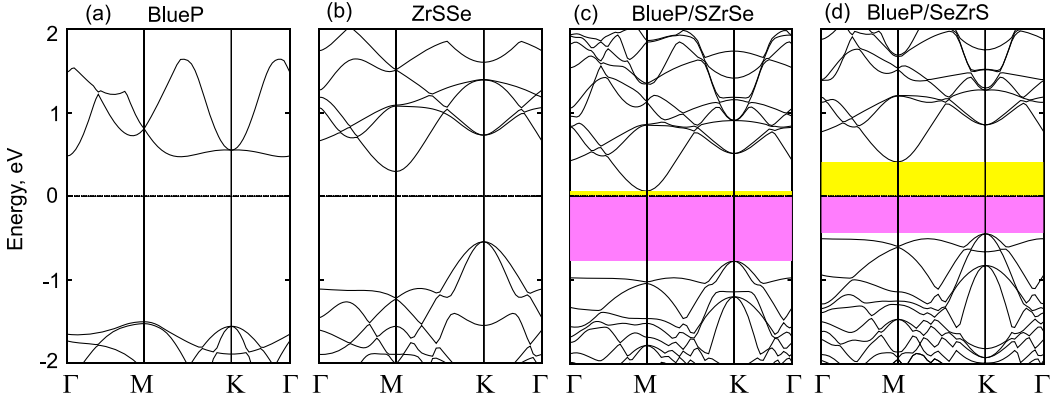


**Fig. 3.** Band structures of (a) monolayer BP, (b) monolayer Janus ZrSSe, (c) BP/SJZ and (d) BP/SeJZ heterostructures.

structure, electronic band structures as well as the phonon dispersion curves of both BP and JZ monolayers are described in Fig. 1. First, our results show that both the BP and JZ monolayers possess a hexagonal unit cell with the lattice parameters of 3.27 Å and 3.74 Å, respectively. These values are comparable with previous measurements [64,65], which confirm the reliability of our computational methods. Moreover, one can find from Fig. 1(b-i) that the atomic structure BP is characterized by the puckered hexagonal crystal structure. Whereas, the JZ monolayer exhibit a layered crystal structure, in which one Zr atom is sandwiched between two different S and Se atoms in both sides, as depicted in Fig. 1(b-ii). At the ground state, we can see that both BP and JZ monolayers displays an indirect band gap nature of semiconductor with the band gap values of 1.97 eV and 0.96 eV, respectively. The conduction band minimum (CB) and valence band maximum (VB) of JZ monolayer are located at  $K$  and  $\Gamma$  point, respectively. Whereas, the CB and VB of BP monolayer are located along the  $K-\Gamma$  path and  $\Gamma-M$  path. Furthermore, it should be noted that traditional DFT approaches, including GGA—PBE are known to underestimate the band gap values of materials, but they can well predict the correct trends and physical mechanism of materials. The phonon dispersion curves of both BP and JZ monolayers, as depicted in Fig. 1(c). The phonon spectra of both

BlueP and Janus ZrSSe show that no imaginary vibrational frequency is observed in the first Brillouin zone, suggesting that monolayers BlueP and Janus ZrSSe are dynamically stable.

We now construct the heterostructures by stacking BP above on top of JZ monolayers. Due to different chalcogen elements S and Se in both sides of JZ monolayer, there are two possible stacking patterns, namely BP/Janus SZrSe (BP/SJZ) and BP/Janus SeZrS (BP/SeJZ), as depicted in Fig. 2. All heterostructures are fully relaxed to obtain the equilibrium interlayer distances  $D_{P,S}$  and  $D_{P,Se}$  for BP/SJZ and BP/SeJZ heterostructures, which are calculated to be 3.44 Å and 3.46 Å, respectively. These values are comparable with those in other BP-based heterostructures [66–68] and Janus-based heterostructures [57,69], which are typical vdW heterostructures. These findings predict that the BP/JZ heterostructures are mainly characterized by the weak vdW interactions. The weak interactions in these heterostructures keep them feasible and thus, they can easily fabricate in practical applications.

We also check the structural stability of such composed heterostructures by calculating the binding energy as follows:

$$E_b = \frac{E_H - E_{BP} - E_{JZ}}{S_0} \quad (1)$$

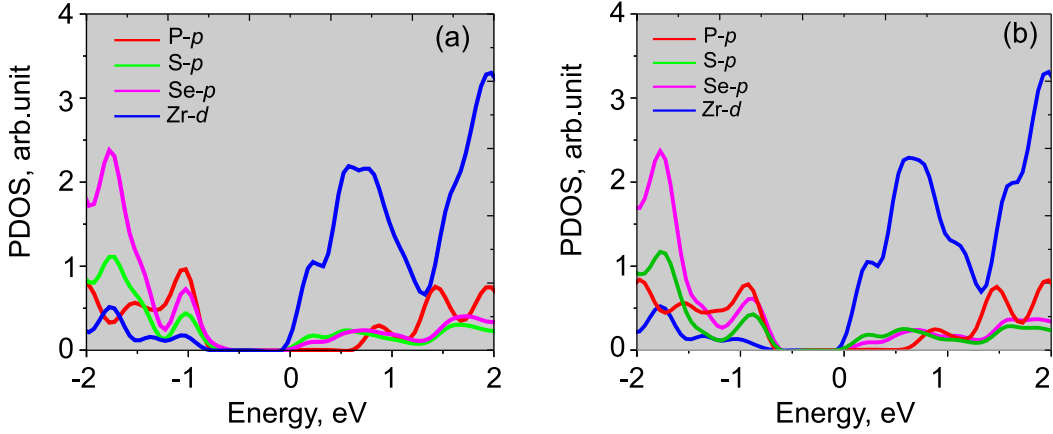


Fig. 4. Projected density of states of (a) BP/SJZ and (c) BP/SeJZ heterostructures.

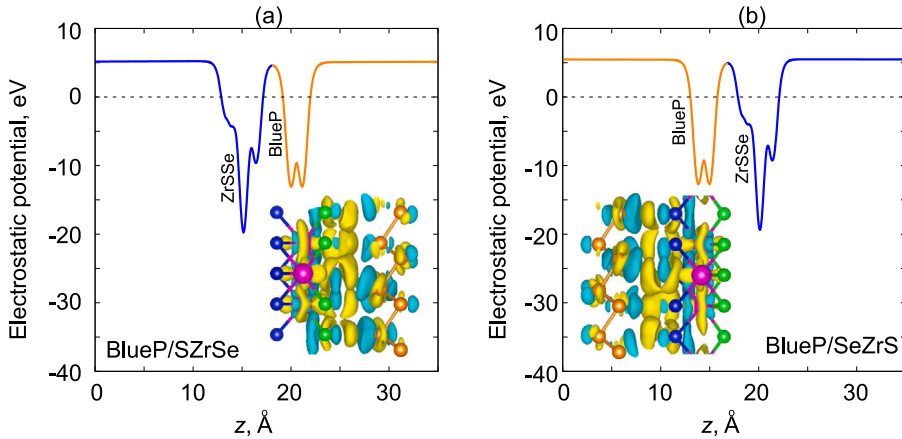


Fig. 5. The electrostatic potential of (a) BP/SJZ and (b) BP/SeJZ heterostructures at the equilibrium state. The inset in Fig. 5(a) and (b) represent the difference in the charge densities. The yellow and cyan regions display the charge accumulation and depletion, respectively. (For interpretation of the references to color in this figure legend, the reader is referred to the web version of this article.)

Here,  $E_H$ ,  $E_{BP}$  and  $E_{JZ}$  are the total energies of composed heterostructures, isolated BlueP and ZrSSe monolayers, respectively.  $S_0$  is the in-plane surface area of heterostructure. At the equilibrium state, the binding energies of BP/SJZ and BP/SeJZ heterostructures are , respectively. The – sign of the binding energies

The electronic band structures of two possible stacking configurations of BP/SJZ and BP/SeJZ heterostructures are presented in Fig. 3 along with those of the isolated constituent BP and Janus ZrSSe supercell. It can be seen that the electronic band structures of BP/SJZ and BP/SeJZ heterostructures are different. Both BP/SJZ and BP/SeJZ heterostructures display the semiconducting character with indirect band gap. However, the CB of the BP/SJZ heterostructure is getting closer to the Fermi level than that of the BP/SeJZ heterostructure. Whereas, the VB of BP/SJZ heterostructure is located far from the Fermi level than that of BP/SeJZ heterostructure. Furthermore, as compared to the band structures of isolated BlueP and ZrSSe supercell, we can find that both the BP/SJZ and BP/SeJZ heterostructures form the type-I band alignment. Both the VB and CB in such heterostructures are contributed by the ZrSSe layer. The type-I band alignment in these heterostructures make them promising candidate for optoelectronic nanodevices such as light-emitting diodes. To confirm the contributions of BlueP and ZrSSe layers in the composed heterostructures, we further calculate and plot the projected density of states (PDOS) of all atoms. These results are depicted in Fig. 4. It can be seen from Fig. 4(a) and Fig. 4(b) that both the VB and CB of the BP/SJZ and (d) BP/SeJZ heterostructures near the Fermi level are contributed mainly by the

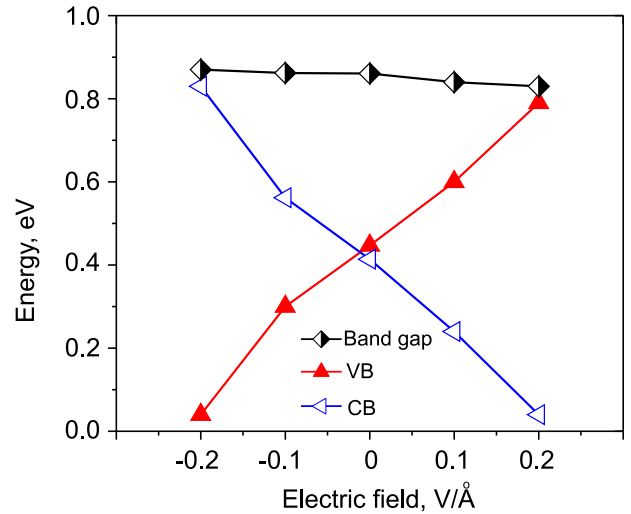


Fig. 6. The variation of the band gap and band alignment of the BP/SeJZ heterostructure under electric field.

ZrSSe layer, confirming the formation of type-I band alignment in these heterostructures.

Furthermore, to check the mechanism of the charge transfer between two layers at the interface, we calculate the difference in charger

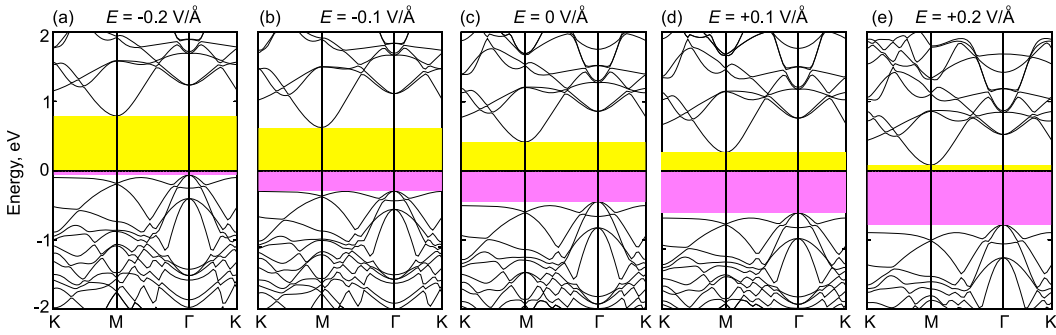


Fig. 7. Band structures of BP/SeJZ heterostructure under different strengths of applied electric field (a).

density as:  $\Delta\rho = \rho_H - \rho_{BP} - \rho_{ZrSSe}$ , where  $\rho_H$ ,  $\rho_{BP}$  and  $\rho_{ZrSSe}$ , respectively, are the charge densities of composed heterostructure, isolated supercell of BlueP and ZrSSe monolayers. The electrostatic potential and the difference in the charge densities of both BP/SJZ and (d) BP/SeJZ heterostructures are illustrated in Fig. 5. In both heterostructures, we can observe that the ZrSSe monolayer has a large potential that the BlueP, resulting in the formation of a large potential drop. Such potential drop demonstrates that a strong electrostatic field may occur in the interface, where BlueP can play a role as an electrode. Moreover, this strong field can affect the dynamics and injection of charge carrier. The difference in charge densities for both cases of heterostructures is depicted in the inset of Fig. 5. One can observe that in both cases of BP/ZrSSe heterostructures, as depicted in the inset of Fig. 5(a) and (b), the yellow region is mainly visualized in the ZrSSe layer, whereas the cyan area is visualized in the BlueP layer. It also demonstrates that the charges are mainly accumulated in the ZrSSe layer, whereas they mainly depleted in the BlueP layer, indicating that the charges are transferred from the BlueP to ZrSSe layer. Our Bader charge calculations also predict that there are only small amount of about 0.032 e and 0.054 e of charges, transferring from BlueP to the ZrSSe layer in the BP/SJZ and BP/SeJZ heterostructures, respectively. Such small charge transfers confirm that the BlueP layer is bonded to the ZrSSe layer via the weak vdW forces. It is interesting that the charge transfer, charge distribution and interface dipole can result in the variation of band gap and band alignment of BlueP/ZrSSe heterostructure. These phenomena have also been confirmed experimentally [70,71].

Furthermore, we investigate the effect of electric field ( $E_{APL}$ ) on the electronic properties and interface characteristics of BP/ZrSSe heterostructures. As above-discussed, the binding energy of BP/SeJZ heterostructure is smaller than that of BP/SJZ heterostructure, indicating that the BP/SeJZ heterostructure is more energetically favorable stacking configuration. Therefore, the BP/SeJZ heterostructure is examined for all our discussions. The dependence of the band gap and band alignment of such heterostructure under the  $E_{APL}$  is plotted in Fig. 6. We can find that the positions of both the VB ( $\Delta_{VB}$ ) and CB ( $\Delta_{CB}$ ) of such heterostructure under electric field are changed linearly. At the equilibrium state, the  $\Delta_{VB}$  and  $\Delta_{CB}$  are calculated to be 0.45 eV and 0.41 eV, respectively. Under the positive  $E_{APL}$ , the  $\Delta_{VB}$  increases up to 0.83 eV at the  $E_{APL} = +0.2$  V/Å, whereas the  $\Delta_{CB}$  decreases down to 0.04 eV. With further increasing the positive  $E_{APL}$ , the  $\Delta_{CB}$  is continuously decreases to be approximately zero, exhibiting the semiconductor to metal transition. On the other hand, under the negative  $E_{APL}$ , the  $\Delta_{VB}$  decreases, whereas the  $\Delta_{CB}$  increases linearly. The transition from semiconductor to metal can achieve in such heterostructure under the negative  $E_{APL}$  of -0.23 V/Å.

The electronic band structures of such heterostructure under different  $E_{APL}$  are illustrated in Fig. 7. One can find that with increasing the  $E_{APL}$  from -0.2 V/Å to +0.2 V/Å, the CB tends to downshift towards the Fermi level, while the VB moves downwards far from the Fermi level. It indicates that the band gap of such heterostructure under electric

field is almost unchanged. However, the electric field can tune the positions of VB and CB relative to the Fermi level. When the strength of applied electric field is about 0.23 V/Å, one of the band edges of such heterostructure crosses the Fermi level, resulting in a conversion from semiconductor to metal.

#### 4. Conclusions

We have constructed the BlueP/ZrSSe heterostructure and explored the stacking and electric field effects on the electronic and interface features of such heterostructures. Our results show that the BlueP/Janus ZrSSe heterostructures exhibit type-I band alignment and possess the indirect band gap nature of semiconductor at the equilibrium state. The stacking configurations affect strongly the band alignment of the heterostructure. Furthermore, the interface properties of such heterostructure can be modulated by applying electric field. The semiconducting character of such heterostructure can be converted into metallic one, making it acceptable for various applications of nanoelectronics and optoelectronics.

#### CRediT authorship contribution statement

**Chuong V. Nguyen:** Conceptualization, Supervision, Writing - original draft, Writing - review & editing, Funding acquisition. **Vo T.T. Vi:** Software, Investigation, Validation. **Le T.T. Phuong:** Methodology, Software, Investigation. **Bui D. Hoi:** Investigation, Validation. **Le T. Hoa:** Investigation, Validation. **Nguyen N. Hieu:** Software, Investigation. **Huynh V. Phuc:** Methodology, Investigation, Validation. **Pham D. Khang:** Software, Investigation, Validation, Writing - original draft.

#### Declaration of competing interest

The authors declare that they have no known competing financial interests or personal relationships that could have appeared to influence the work reported in this paper.

#### Acknowledgment

This research is funded by Vietnam National Foundation for Science and Technology Development (NAFOSTED) under grant number 103.01-2019.05.

#### References

- [1] A.C. Neto, F. Guinea, N.M. Peres, K.S. Novoselov, A.K. Geim, The electronic properties of graphene, *Rev. Modern Phys.* 81 (1) (2009) 109.
- [2] C. González-Santander, F. Domínguez-Adame, M. Hilke, R.A. Roemer, Localisation and finite-size effects in graphene flakes, *Europhys. Lett.* 104 (1) (2013) 17012.

- [3] N. Wilson, P. Pandey, R. Beanland, J. Rourke, U. Lupo, G. Rowlands, R. Römer, On the structure and topography of free-standing chemically modified graphene, *New J. Phys.* 12 (12) (2010) 125010.
- [4] Z. Cai, B. Liu, X. Zou, H.-M. Cheng, Chemical vapor deposition growth and applications of two-dimensional materials and their heterostructures, *Chem. Rev.* 118 (13) (2018) 6091–6133.
- [5] G. Fiori, F. Bonaccorso, G. Iannaccone, T. Palacios, D. Neumaier, A. Seabaugh, S.K. Banerjee, L. Colombo, Electronics based on two-dimensional materials, *Nat. Nanotechnol.* 9 (10) (2014) 768.
- [6] F. Koppens, T. Mueller, P. Avouris, A. Ferrari, M. Vitiello, M. Polini, Photodetectors based on graphene, other two-dimensional materials and hybrid systems, *Nat. Nanotechnol.* 9 (10) (2014) 780.
- [7] B. Mendoza-Sánchez, Y. Gogotsi, Synthesis of two-dimensional materials for capacitive energy storage, *Adv. Mater.* 28 (29) (2016) 6104–6135.
- [8] Y. Kubota, K. Watanabe, O. Tsuda, T. Taniguchi, Deep ultraviolet light-emitting hexagonal boron nitride synthesized at atmospheric pressure, *Science* 317 (5840) (2007) 932–934.
- [9] G. Cassabois, P. Valvin, B. Gil, Hexagonal boron nitride is an indirect bandgap semiconductor, *Nat. Photonics* 10 (4) (2016) 262.
- [10] A. Carvalho, M. Wang, X. Zhu, A.S. Rodin, H. Su, A.H.C. Neto, Phosphorene: from theory to applications, *Nat. Rev. Mater.* 1 (11) (2016) 1–16.
- [11] Z. Ma, B. Wang, L. Ou, Y. Zhang, X. Zhang, Z. Zhou, Structure and properties of phosphorene-like IV-VI 2D materials, *Nanotechnology* 27 (41) (2016) 415203.
- [12] H.-P. Komsa, J. Kotakoski, S. Kurasch, O. Lehtinen, U. Kaiser, A.V. Krasheninnikov, Two-dimensional transition metal dichalcogenides under electron irradiation: defect production and doping, *Phys. Rev. Lett.* 109 (3) (2012) 035503.
- [13] D. Jariwala, V.K. Sangwan, L.J. Lauhon, T.J. Marks, M.C. Hersam, Emerging device applications for semiconducting two-dimensional transition metal dichalcogenides, *ACS Nano* 8 (2) (2014) 1102–1120.
- [14] Q.H. Wang, K. Kalantar-Zadeh, A. Kis, J.N. Coleman, M.S. Strano, Electronics and optoelectronics of two-dimensional transition metal dichalcogenides, *Nat. Nanotechnol.* 7 (11) (2012) 699.
- [15] H. Wang, H. Yuan, S.S. Hong, Y. Li, Y. Cui, Physical and chemical tuning of two-dimensional transition metal dichalcogenides, *Chem. Soc. Rev.* 44 (9) (2015) 2664–2680.
- [16] S. Wang, J. Wang, Spin and valley half-metal state in MoS<sub>2</sub> monolayer, *Physica B* 458 (2015) 22–26.
- [17] Y. Zhang, J. Liu, G. Wu, W. Chen, Porous graphitic carbon nitride synthesized via direct polymerization of urea for efficient sunlight-driven photocatalytic hydrogen production, *Nanoscale* 4 (17) (2012) 5300–5303.
- [18] K. Srinivasu, B. Modak, S.K. Ghosh, Porous graphitic carbon nitride: a possible metal-free photocatalyst for water splitting, *J. Phys. Chem. C* 118 (46) (2014) 26479–26484.
- [19] Y. Luo, S. Wang, S. Li, Z. Sun, J. Yu, W. Tang, M. Sun, Transition metal doped puckered arsenene: Magnetic properties and potential as a catalyst, *Physica E* 108 (2019) 153–159.
- [20] Z. Cui, K. Bai, X. Wang, E. Li, J. Zheng, Electronic, magnetism, and optical properties of transition metals adsorbed g-GaN, *Physica E* 118 (2020) 113871.
- [21] Z. Li, J. Li, C. He, T. Ouyang, C. Zhang, S. Zhang, C. Tang, R.A. Römer, J. Zhong, Few-layer  $\rho$ -SnSe with strong visible light absorbance and ultrahigh carrier mobility, *Phys. Rev. A* 13 (1) (2020) 014042.
- [22] Z. Li, X. Shi, C. He, T. Ouyang, J. Li, C. Zhang, S. Zhang, C. Tang, R.A. Römer, J. Zhong, Ge3P2: new viable two-dimensional semiconductors with ultrahigh carrier mobility, *Appl. Surf. Sci.* 497 (2019) 143803.
- [23] S.Y. Zhou, G.-H. Gweon, A. Fedorov, P.N.D. First, W. De Heer, D.-H. Lee, F. Guinea, A.C. Neto, A. Lanzara, Substrate-induced bandgap opening in epitaxial graphene, *Nature Mater.* 6 (10) (2007) 770–775.
- [24] K.F. Mak, C. Lee, J. Hone, J. Shan, T.F. Heinz, Atomically thin MoS<sub>2</sub>: a new direct-gap semiconductor, *Phys. Rev. Lett.* 105 (13) (2010) 136805.
- [25] B. Radisavljevic, A. Radenovic, J. Brivio, V. Giacometti, A. Kis, Single-layer MoS<sub>2</sub> transistors, *Nat. Nanotechnol.* 6 (3) (2011) 147.
- [26] X. Zhou, N. Zhou, C. Li, H. Song, Q. Zhang, X. Hu, L. Gan, H. Li, J. Lü, J. Luo, et al., Vertical heterostructures based on SnSe<sub>2</sub>/MoS<sub>2</sub> for high performance photodetectors, *2D Mater.* 4 (2) (2017) 025048.
- [27] Z. Ben Aziza, H. Henck, D. Pierucci, M.G. Silly, E. Lhuillier, G. Patriarche, F. Sirotti, M. Eddrief, A. Ouerghi, Van der waals epitaxy of GaSe/graphene heterostructure: electronic and interfacial properties, *ACS Nano* 10 (10) (2016) 9679–9686.
- [28] H. Coy Diaz, J. Avila, C. Chen, R. Addou, M.C. Asensio, M. Batzill, Direct observation of interlayer hybridization and dirac relativistic carriers in graphene/MoS<sub>2</sub> van der waals heterostructures, *Nano Lett.* 15 (2) (2015) 1135–1140.
- [29] Z.B. Aziza, H. Henck, D. Di Felice, D. Pierucci, J. Chaste, C.H. Naylor, A. Balan, Y.J. Dappe, A.C. Johnson, A. Ouerghi, Bandgap inhomogeneity of MoS<sub>2</sub> monolayer on epitaxial graphene bilayer in van der waals pn junction, *Carbon* 110 (2016) 396–403.
- [30] T.V. Vu, N.V. Hieu, H.V. Phuc, N.N. Hieu, H. Bui, M. Idrees, B. Amin, C.V. Nguyen, Graphene/WSeTe van der Waals heterostructure: Controllable electronic properties and schottky barrier via interlayer coupling and electric field, *Appl. Surf. Sci.* 507 (2020) 145036.
- [31] B. Yang, M.-F. Tu, J. Kim, Y. Wu, H. Wang, J. Alicea, R. Wu, M. Bockrath, J. Shi, Tunable spin-orbit coupling and symmetry-protected edge states in graphene/WSe<sub>2</sub>, *2D Mater.* 3 (3) (2016) 031012.
- [32] J. Tan, A. Avsar, J. Balakrishnan, G. Koon, T. Taychatanapat, E. O'Farrell, K. Watanabe, T. Taniguchi, G. Eda, A. Castro Neto, et al., Electronic transport in graphene-based heterostructures, *Appl. Phys. Lett.* 104 (18) (2014) 183504.
- [33] W. Zhang, Y. Zeng, N. Xiao, H.H. Hng, Q. Yan, One-step electrochemical preparation of graphene-based heterostructures for Li storage, *J. Mater. Chem.* 22 (17) (2012) 8455–8461.
- [34] K.D. Pham, N.N. Hieu, H.V. Phuc, I. Fedorov, C. Duque, B. Amin, C.V. Nguyen, Layered graphene/GaS van der Waals heterostructure: Controlling the electronic properties and schottky barrier by vertical strain, *Appl. Phys. Lett.* 113 (17) (2018) 171605.
- [35] Q. Lv, R. Lv, Two-dimensional heterostructures based on graphene and transition metal dichalcogenides: Synthesis, transfer and applications, *Carbon* 145 (2019) 240–250.
- [36] Y. Luo, S. Wang, K. Ren, J.-P. Chou, J. Yu, Z. Sun, M. Sun, Transition-metal dichalcogenides/Mg(OH)<sub>2</sub> van der Waals heterostructures as promising water-splitting photocatalysts: a first-principles study, *Phys. Chem. Chem. Phys.* 21 (4) (2019) 1791–1796.
- [37] W. Choi, I. Akhtar, D. Kang, Y.-j. Lee, J. Jung, Y.H. Kim, C.-H. Lee, D.J. Hwang, Y. Seo, Optoelectronics of multijunction heterostructures of transition metal dichalcogenides, *Nano Lett.* 20 (3) (2020) 1934–1943.
- [38] J. Du, C. Xia, W. Xiong, T. Wang, Y. Jia, J. Li, Two-dimensional transition-metal dichalcogenides-based ferromagnetic van der waals heterostructures, *Nanoscale* 9 (44) (2017) 17585–17592.
- [39] S. Wang, H. Tian, C. Ren, J. Yu, M. Sun, Electronic and optical properties of heterostructures based on transition metal dichalcogenides and graphene-like zinc oxide, *Sci. Rep.* 8 (1) (2018) 1–6.
- [40] T.V. Vu, N.V. Hieu, L.T. Thao, N.N. Hieu, H.V. Phuc, H. Bui, M. Idrees, B. Amin, L.M. Duc, C.V. Nguyen, Tailoring the structural and electronic properties of an SnSe<sub>2</sub>/MoS<sub>2</sub> van der Waals heterostructure with an electric field and the insertion of a graphene sheet, *Phys. Chem. Chem. Phys.* 21 (39) (2019) 22140–22148.
- [41] S. Wang, C. Ren, H. Tian, J. Yu, M. Sun, MoS<sub>2</sub>/ZnO van der Waals heterostructure as a high-efficiency water splitting photocatalyst: a first-principles study, *Phys. Chem. Chem. Phys.* 20 (19) (2018) 13394–13399.
- [42] Y. Luo, K. Ren, S. Wang, J.-P. Chou, J. Yu, Z. Sun, M. Sun, First-principles study on Transition-Metal Dichalcogenide/BSe van der Waals heterostructures: A promising water-splitting photocatalyst, *J. Phys. Chem. C* 123 (37) (2019) 22742–22751.
- [43] Z. Cui, K. Ren, Y. Zhao, X. Wang, H. Shu, J. Yu, W. Tang, M. Sun, Electronic and optical properties of van der waals heterostructures of g-GaN and transition metal dichalcogenides, *Appl. Surf. Sci.* 492 (2019) 513–519.
- [44] K. Ren, S. Wang, Y. Luo, J.-P. Chou, J. Yu, W. Tang, M. Sun, High-efficiency photocatalyst for water splitting: a Janus MoSe<sub>X</sub>N (X= Ga, Al) van der waals heterostructure, *J. Phys. D: Appl. Phys.* 53 (18) (2020) 185504.
- [45] J.L. Zhang, S. Zhao, C. Han, Z. Wang, S. Zhong, S. Sun, R. Guo, X. Zhou, C.D. Gu, K.D. Yuan, et al., Epitaxial growth of single layer blue phosphorus: a new phase of two-dimensional phosphorus, *Nano Lett.* 16 (8) (2016) 4903–4908.
- [46] A.-Y. Lu, H. Zhu, J. Xiao, C.-P. Chuu, Y. Han, M.-H. Chiu, C.-C. Cheng, C.-W. Yang, K.-H. Wei, Y. Yang, et al., Janus monolayers of transition metal dichalcogenides, *Nat. Nanotechnol.* 12 (8) (2017) 744–749.
- [47] L. Zhu, S.-S. Wang, S. Guan, Y. Liu, T. Zhang, G. Chen, S.A. Yang, Blue phosphorene oxide: strain-tunable quantum phase transitions and novel 2d emergent fermions, *Nano Lett.* 16 (10) (2016) 6548–6554.
- [48] S.-D. Guo, J. Dong, Biaxial strain tuned electronic structures and power factor in janus transition metal dichalcogenide monolayers, *Semicond. Sci. Technol.* 33 (8) (2018) 085003.
- [49] H. Liu, Z. Huang, C. He, Y. Wu, L. Xue, C. Tang, X. Qi, J. Zhong, Strain engineering the structures and electronic properties of janus monolayer transition-metal dichalcogenides, *J. Appl. Phys.* 125 (8) (2019) 082516.
- [50] B. Sa, Y.-L. Li, J. Qi, R. Ahuja, Z. Sun, Strain engineering for phosphorene: the potential application as a photocatalyst, *J. Phys. Chem. C* 118 (46) (2014) 26560–26568.
- [51] Q. Yang, W. Xiong, L. Zhu, G. Gao, M. Wu, Chemically functionalized phosphorene: two-dimensional multiferroics with vertical polarization and mobile magnetism, *J. Am. Chem. Soc.* 139 (33) (2017) 11506–11512.
- [52] X. Ma, X. Yong, C.-c. Jian, J. Zhang, Transition metal-functionalized Janus MoS<sub>2</sub> monolayer: A magnetic and efficient single-atom photocatalyst for water-splitting applications, *J. Phys. Chem. C* 123 (30) (2019) 18347–18354.

- [53] A.B. Maghirang, Z.-Q. Huang, R.A.B. Villaos, C.-H. Hsu, L.-Y. Feng, E. Florido, H. Lin, A. Bansil, F.-C. Chuang, Predicting two-dimensional topological phases in janus materials by substitutional doping in transition metal dichalcogenide monolayers, *npj 2D Mater. Appl.* 3 (1) (2019) 1–8.
- [54] M. Sun, J.-P. Chou, J. Yu, W. Tang, Electronic properties of blue phosphorene/graphene and blue phosphorene/graphene-like gallium nitride heterostructures, *Phys. Chem. Chem. Phys.* 19 (26) (2017) 17324–17330.
- [55] Q. Peng, Z. Waing, B. Sa, B. Wu, Z. Sun, Blue phosphorene/MS<sub>2</sub> (M = Nb, Ta) heterostructures as promising flexible anodes for lithium-ion batteries, *ACS Appl. Mater. Interfaces* 8 (21) (2016) 13449–13457.
- [56] D.D. Vo, T.V. Vu, N.V. Hieu, N.N. Hieu, H.V. Phuc, N.T. Binh, L.T. Phuong, M. Idrees, B. Amin, C.V. Nguyen, Band alignment and optical features in Janus-MoSeTe/X(OH)<sub>2</sub> (X = Ca, Mg) van der Waals heterostructures, *Phys. Chem. Chem. Phys.* 21 (46) (2019) 25849–25858.
- [57] D. Chen, X. Lei, Y. Wang, S. Zhong, G. Liu, B. Xu, C. Ouyang, Tunable electronic structures in BP/MoS<sub>2</sub> van der Waals heterostructures by external electric field and strain, *Appl. Surf. Sci.* 497 (2019) 143809.
- [58] X. Li, X. Wang, W. Hao, C. Mi, H. Zhou, Structural, electronic, and electromechanical properties of MoS<sub>2</sub>/blue phosphorene heterobilayer, *AIP Adv.* 9 (11) (2019) 115302.
- [59] J. Zhang, S. Jia, I. Kholmanov, L. Dong, D. Er, W. Chen, H. Guo, Z. Jin, V.B. Shenoy, L. Shi, et al., Janus monolayer transition-metal dichalcogenides, *ACS Nano* 11 (8) (2017) 8192–8198.
- [60] Z. Zeng, Z. Yin, X. Huang, H. Li, Q. He, G. Lu, F. Boey, H. Zhang, Single-layer semiconducting nanosheets: High-yield preparation and device fabrication, *Angew. Chem. Int. Ed.* 50 (47) (2011) 11093–11097.
- [61] P. Giannozzi, S. Baroni, N. Bonini, M. Calandra, R. Car, C. Cavazzoni, D. Ceresoli, G.L. Chiarotti, M. Cococcioni, I. Dabo, A.D. Corso, S. de Gironcoli, S. Fabris, G. Fratesi, R. Gebauer, U. Gerstmann, C. Gougaussis, A. Kokalj, M. Lazzeri, L. Martin-Samos, N. Marzari, F. Mauri, R. Mazzarello, S. Paolini, A. Pasquarello, L. Paulatto, C. Sbraccia, S. Scandolo, G. Sclauzero, A.P. Seitsonen, A. Smogunov, P. Umari, R.M. Wentzcovitch, QUANTUM ESPRESSO: a modular and open-source software project for quantum simulations of materials, *J. Phys.: Condens. Matter* 21 (39) (2009) 395502.
- [62] P. Giannozzi, O. Andreussi, T. Brumme, O. Bunau, M.B. Nardelli, M. Calandra, R. Car, C. Cavazzoni, D. Ceresoli, M. Cococcioni, N. Colonna, I. Carnimeo, A.D. Corso, S. de Gironcoli, P. Delugas, R.A. DiStasio, A. Ferretti, A. Floris, G. Fratesi, G. Fugallo, R. Gebauer, U. Gerstmann, F. Giustino, T. Gorni, J. Jia, M. Kawamura, H.-Y. Ko, A. Kokalj, E. Küçükbenli, M. Lazzeri, M. Marsili, N. Marzari, F. Mauri, N.L. Nguyen, H.-V. Nguyen, A.O. de-la Roza, L. Paulatto, S. Poncé, D. Rocca, R. Sabatini, B. Santra, M. Schlipf, A.P. Seitsonen, A. Smogunov, I. Timrov, T. Thonhauser, P. Umari, N. Vast, X. Wu, S. Baroni, Advanced capabilities for materials modelling with quantum ESPRESSO, *J. Phys.: Condens. Matter* 29 (46) (2017) 465901.
- [63] S. Grimme, Semiempirical GGA-type density functional constructed with a long-range dispersion correction, *J. Comput. Chem.* 27 (15) (2006) 1787–1799.
- [64] G. Barik, S. Pal, Energy gap-modulated blue phosphorene as flexible anodes for lithium-and sodium-ion batteries, *J. Phys. Chem. C* 123 (5) (2019) 2808–2819.
- [65] S.-D. Guo, Y.-F. Li, X.-S. Guo, Predicted janus monolayer ZrS<sub>2</sub> with enhanced n-type thermoelectric properties compared with monolayer ZrS<sub>2</sub>, *Comput. Mater. Sci.* 161 (2019) 16–23.
- [66] H. Lin, R. Jin, S. Zhu, Y. Huang, C<sub>3</sub>N/blue phosphorene heterostructure as a high rate-capacity and stable anode material for lithium ion batteries: Insight from first principles calculations, *Appl. Surf. Sci.* 505 (2020) 144518.
- [67] Y. Wang, N. Song, X. Yang, J. Zhang, B. Xu, M. Li, Y. Zheng, D. Yang, Tailoring the electronic properties of graphyne/blue phosphorene heterostructure via external electric field and vertical strain, *Chem. Phys. Lett.* 730 (2019) 277–282.
- [68] Y. Wei, F. Wang, W. Zhang, X. Zhang, The electric field modulation of electronic properties in a type-II phosphorene/PbI<sub>2</sub> van der Waals heterojunction, *Phys. Chem. Chem. Phys.* 21 (15) (2019) 7765–7772.
- [69] K.D. Pham, N.N. Hieu, H.V. Phuc, B.D. Hoi, V.V. Ilysov, B. Amin, C.V. Nguyen, First principles study of the electronic properties and schottky barrier in vertically stacked graphene on the janus moses under electric field, *Comput. Mater. Sci.* 153 (2018) 438–444.
- [70] F. Ceballos, M.Z. Bellus, H.-Y. Chiu, H. Zhao, Probing charge transfer excitons in a MoSe<sub>2</sub>-WS<sub>2</sub> van der waals heterostructure, *Nanoscale* 7 (41) (2015) 17523–17528.
- [71] S. Tongay, W. Fan, J. Kang, J. Park, U. Koldemir, J. Suh, D.S. Narang, K. Liu, J. Ji, J. Li, et al., Tuning interlayer coupling in large-area heterostructures with CVD-grown MoS<sub>2</sub> and WS<sub>2</sub> monolayers, *Nano Lett.* 14 (6) (2014) 3185–3190.